Gas Processing Journal

Vol. 10, No. 2, 2022, pp. 13 - 24
http://gpj.ui.ac.ir

Research Paper

# Developing a model for calculating pure gas thermal conductivity at P=1bar using particle swarm optimization algorithm

**Amirhossein Oudi[1], Samaneh Faramarzi[2], Shiva Yarmohammadian[2], Yegane Davoodbeygi[3*]**

[1] Department of Chemical Engineering, Faculty of Engineering, University of Kashan, Kashan, Iran
[2] Department of Chemical Engineering, Faculty of Engineering, Razi University, Kermanshah, Iran
[3] Department of Chemical Engineering, University of Hormozgan, Bandar Abbas, Iran

Received: 2022-05-26 Revised: 2022-10-14 Accepted: 2022-11-27

**Abstract:** One of the most crucial variables in the study of heat transport is thermal conductivity and methods for measuring this variable have long been sought after. In this paper, to achieve the equation for approximation of the thermal conductivity coefficient, 61 experimental data were collected for pure gases in P=1 bar and variable temperature (91.88-1500 K). The proposed model was then obtained using the Particle Swarm Optimization (PSO) algorithm in MATLAB V2015. It includes a variety of hydrocarbon and non-hydrocarbon compounds. The physical properties of pure gases including temperature, critical temperature, critical pressure, molecular weight, viscosity, and heat capacity at constant volume were obtained for pure components and used for prediction of the conductivity of these gases. Also, during the validation phase, the suggested model attained the most accurate prediction withR^2=0.9995. This model is capable of predicting the thermal conductivity coefficient of gases with a mean relative error percentage of 4.67% and mean square error percentage of 2.4210×10-4% compared to actual data. These results are significantly better than those obtained from other models.

**keywords:** heat transfer, thermal conductivity, pure gas, particle swarm optimization algorithm.

## 1. Introduction

Conductive form of heat transfer is the transmission of heat using molecular motion in a stationary substance and occurs mainly in solids or stationary environments such as stationary liquids. Conductive heat transfer of gases and liquids is because of the collision and diffusion during the random mobility of molecules. On the other hand, energy transfer by free electrons and molecular network vibrations combine to create heat transfer in solids [1]. Thermal conductivity is a property of a material that proclaims its ability to conduct heat [2].

Even at high pressures, accurate measurement equipment can determine the thermal conductivity of gases with an accuracy of less than 1%. The measurement of thermal conductivity for the noble gases He and Ar at low densities is consistent with the kinetic theory's predictions, and similar outcomes are anticipated for Ne, Kr, and Xe [3]. Numerous gases have had their thermal conductivity measured over history and compiled. Table 1 shows an overview of the background of the studies conducted on the measurement and prediction of the conductivity coefficient of pure fluids and mixture fluids.

**Table 1. A list of techniques and correlations used to predict thermal conductivity**

| Source | Comment | Year | Reference |
|---|---|---|---|
| Ubbelohde | He believed that chemical species might be thought of as dilute gas molecules in various energy states and that the diffusion of these species is what causes an energy flux. | 1935 | [4] |
| Pidduck | Pidduck was the first to use the Chapman-Enskog method for an infinitely diluted gas of spherical molecules in the case of ideally rough stiff elastic | 1953 | [5] |

* Corresponding Author.
Authors' Email Address: [1] **H. Amidzadeh** (hadi.amidzadeh8@gmail.com), [2] **E. Nemati Lay** (enemati@kashanu.ac.ir), [3] **A. Mohebbi** (alireza2010mh@gmail.com), [4] **E. Kamali** (erfan.kamali7396@gmail.com)



http://dx.doi.org/10.22108/GPJ.2023.135773.1126

| | | | |
|---|---|---|---|
| | spherical molecules having rotational energy that could be converted into translational energy. This was the first instance when a polyatomic molecule scenario had been fully investigated. | | |
| The Eucken approximation | He understood how the internal degree of freedom affected the conductivity of a diluted gas containing polyatomic molecules and how the specific heat ratio relates to this. | 1954 | [6] |
| Theory of Longuet-Higgins and Pople | Using the single collisional mechanism assumption, Longuet-Higgins and Pople estimated the conductivity in a dense gas of hard spheres. | 1956 | [7] |
| Theory of Longuet-Higgins and Valleau | They thought about how a square-well potential affects the interactions between molecules. | 1958 | [8] |
| Choh and Uhlenbeck | These theories produce formulas for conductivity in terms of a series expansion in the density and are frequently based on density expansions of a generalized Boltzmann equation. | 1958 | [9] |
| Srivastava and Barua | The thermal conductivity of binary mixtures including $O_2$-He, $O_2$-Ne, $O_2$-Kr, and $O_2$-Xe at 30 and 45 °C for different compounds was measured through a thick-set hot cord. For pure $O_2$, the experimental amount of thermal conductivity is less than that proposed by Hirschfelder's recent theory based on the supposition of local chemical equilibrium. | 1960 | [10] |
| Theory of Davis et al. | In a more thorough analysis of the transport characteristics of a square-well fluid, Davis et al. computed the convective and collisional contributions using a modified Boltzmann equation. | 1961 | [11] |
| Bogolubov | These theories produce formulas for conductivity in terms of a series expansion in the density and are based on density expansions of an extended Boltzmann equation. | 1962 | [12] |
| Theory of Horrocks and McLaughlin | Using frequency as a measure of conductivity, they proposed the face-centered cubic lattice shape. | 1963 | [13] |
| Cohen | These theories generate formulas for conductivity that are based on density expansions of a generalized Boltzmann equation in terms of a series. | 1965 | [14] |
| Theory of Sengers | His analysis takes into account Longuet-Higgins and Valleau's omitted effect of the distribution function disturbance from the local equilibrium value. | 1966 | [15] |
| Mathur et al. | Thermal conductivity data for Ne-Ar, Ne-Kr, Ar-Xe, and Kr-Xe systems have been recited as a dependent of percentage composition at temperatures of 40, 65, and 90 °C. Similar results have been obtained for the Kr - Ar - Ne, Xe - Kr - Ar triple systems, and an Xe - Kr - Ar -Ne quaternary system. In this method, a conductive cell of a kind of thick hot wire was used. A similar study has been done for triple and quadruple mixtures and good results have been obtained about the partial suitability of various methods for calculating the thermal conductivity of multicomponent mixtures of gases | 1967 | [16] |
| Theory of Enskog | Enskog considered the example of hard spheres to make the first significant contribution to the calculation of the conductivity of a dense gas. | 1970 | [17] |
| De Groot et al | They described new precision and estimation of the thermal conductivity of gases in the pressure and temperature ranges of 1 to 400 atm and 25 to 800 °C, respectively | 1974 | [18] |
| Healy et al. | They investigated the thermal conductivity of four different pure monoatomic gases including He, Ne, Ar, and Kr. The evaluation was made at room temperature on a high-accuracy instrument with a hot wire. The thermal conductivity of Ne, Ar, and Kr has been analyzed as a function of density | 1976 | [19] |
| Plinski | A correlation was used to calculate the thermal conductivity of CO, $CO_2$, $N_2$, He, Xe, CO, $O_2$, and | 2001 | [20] |

| | | | |
|---|---|---|---|
| | Ar as a function of temperature. | | |
| Mao-Gang He et al. | For halogenated hydrocarbon refrigerants, they proposed a new correlation to measure the thermal conductivity of the dense fluid. | 2002 | [21] |
| Eslamloueyan and Khademi. | The variables of the proposed ANN model were molecular weight, critical temperature, and critical pressure. The use of this model for the tested data suggests that the thermal conductivity of pure gases at atmospheric pressure can be predicted by a significant relative error and less than other alternative correlations. | 2009 | [22] |
| Gauthier et al | They developed a novel experimental method using a three-setup to measure the thermal conductivity of a gas. The purpose of this study was to confirm the 3 method's simplicity and convenience of use. It was possible to measure the thermal conductivities of both pure gases and mixtures of gases with high reproducibility and a variability of less than 5%. When evaluated at 298 K and atmospheric pressure, the thermal conductivity of various pure gases, including nitrogen, helium, and carbon dioxide, was compared to reference levels with an error of less than 5%. | 2013 | [23] |
| Ribeiro et al. | A novel method of estimating heat transfer coefficients for a gas-solid interface was proposed, in which the photon, even when radiation with a low frequency is transmitted, consists of electronic transitions rather than passing instantly through the wall of gases and solids. The Landau-Teller model determines the delay necessary for electron transmission, which is crucial to the process of heat transfer. | 2017 | [24] |
| Lang et al. | They created a technique for determining how thermally conductive combinations of pressurized gases are. They employ a mixture of carbon dioxide and PDMS, a linear polymer with a molecular weight of 11000 g/mol. Experiments were conducted at 25, 40, and 60℃ and up to 16 MPa. | 2019 | [25] |
| Cardona and Valderrama | They recently suggested a generalized equation of state that correlates and predicts various physical and transport properties of ionic liquids, such as thermal conductivity and speed of sound, and only has one changeable parameter. | 2020 | [26] |
| Li et al. | The thermal conductivity of $H_2/CO_2$ binary mixtures were measured using a system based on the short-hot-wire method at 323.15-620.05 K and 2.14-9.37 MPa. | 2020 | [27] |
| Kim et al. | Using a transient hot-wire technique, thermal conductivity measurements of pure R1243zf and binary mixes of R32 + R1243zf and R32 + R1234yf were made in the homogenous liquid and vapour phases. The relative differences between the calculated thermal conductivities using the extended corresponding states (ECS) model and the measured thermal conductivities. | 2021 | [28] |
| Liu et al. | They simulate the thermal conductivity of HFCs, HFOs, and their binary mixtures using the RES method and the CPA equation of state. Except the near-critical zone, the dependence of the thermal conductivity on the thermodynamic state is reduced to a univariate function of residual entropy throughout a wide range of temperatures and pressure. | 2021 | [29] |
| Dehlouz et al. | Rosenfeld's original entropy scaling method was modified to compute the thermal conductivities of pure fluids. A function of the Tv-residual was connected to a specially developed expression for decreased thermal conductivity. | 2022 | [30] |
| Yu Liu et.al | To represent the thermal conductivity of HFC, HFO, and HCFO refrigerants in a liquid phase, a semi-empirical model was developed. The Peng-Robinson Equation of State (PR equation) and the Modified | 2022 | [31] |

| | | | |
|---|---|---|---|
| | Enskog Theory (MET) model served as the foundation for the suggested thermal conductivity model, which also included an empirical adjustment to the MET model's cross-contribution factor to increase precision. | | |
| Niksirat et al. | Their model was used for binary and multicomponent liquid phase combinations and was tested on pure HCFCs, HFCs, and HFOs. | 2022 | [32] |
| Rottmann and Beikircher | The effective thermal conductivity of pure and opaque expanded perlite was investigated at gas pressures between 104 hPa and 103 hPa and temperatures between 293 K and 1073 K using guarded hot plates and transient hot wire measurements. The description of the coupling effect between solid-body and gas heat conduction was improved by the addition of a single novel coupling parameter to the model, which expresses the exceedance of the gas pressure-dependent contribution of the effective thermal conductivity relative to the thermal conductivity of the gas inside the pores. | 2022 | [33] |

When the complications of issues arise, the experimental data must be estimated. Traditional optimization algorithms may find it hard to meet the supplies of the problems which leads to new influential algorithms [34]. Over the past few years, various traditional novelty algorithms have been developed as impressive and practical approaches to problem optimization [35, 36]. due to the continuous improvement of computing power. By using numerical integration, they aimed to quickly optimize the reaction rate, and conversion range, and accommodate any collection of differential rate equations [37]. Particle swarm optimization (PSO) and genetic algorithm (GA) are the most hopeful algorithms for network optimization [38]. PSO as an evolutionary random algorithm, that is nature-inspired, is evoked by the public behavior of organisms, which warrants a coordinated swarm to achieve the ideal result extended by Kennedy and Eberhart [39]. It is randomly placed in the workspace, and each particle's objective function quantity is assessed [40]. Like GA, PSO is an optimization tool which is based on population. But, GA and PSO are different in some ways: (1) PSO has various evolutionary mechanisms, with the exception of genetic agents such as crosses and mutations, which update their PSO particles at internal speeds. (2) At the same time, particles of PSO have a memory that is vital for the algorithm [41].

In recent years, the PSO optimization was used in the nonlinear Regression in problems such as model design and parameter estimation for the thermodynamics, kinetics, and hydrodynamics of mixed salt precipitation in porous media [42], interacting parameter correlation in the Wilson, NRTL, and UNIQUAC models [43], toxic vapours' kinetic adsorption on activated carbon in the batch reactor [44], predict crude oil properties [45], for the gas cross flow in packed bed reactors, a novel Sauter mean diameter correlation has been developed [46], and an innovative theoretical and practical approach based on friction volume theory and friction theory parameter tweaking for viscosity-sensitive Iranian heavy crude oils [47].

In previous studies, relationships have been proposed to obtain thermal conductivity, which are mostly complex and detailed, and there are some difficulties in using them. In this study, an optimum and simple model with a low error rate of specific gases is proposed by PSO using data related to the physical properties of gas in 1 bar.

## 2. Methodology

### 2.1. PSO algorithm

James Kennedy and Russell Eberhart [48] presented the PSO technique in 1995. This algorithm is adapted from the collective performance of a collection of animals such as fliers and fish. PSO is an optimization approach based on population inspired by the public treatment of birds or fish training. It sometimes bears many similarities to Evolutionary Calculation techniques (EC), Genetic Algorithms (GA), and Evolutionary Strategies (ES). But there are also many contrasts between these methods [49]. The PSO starts with a collection of chance iotas (solutions) and therefore takes optimal search by keeping generations up to date by coursing the best valuations in every iterance, in which every particle is kept up to date. The first of these values is the foremost fit ($x^{i,pbest}[t]$). This foremost value is the best in the world and is entitled ($x^{gbest}[t]$ ). After gaining the two foremost values, the particle keeps its velocity and position up to date using the following equations:

$$v^i[t+1] = wv^i[t] + c_1r_1(x^{i,pbest}[t] - x^i[t]) + c_2r_2(x^{gbest}[t] - x^i[t]) \quad (1)$$

$$x^i[t+1] = x^i[t] + v^i[t+1] \quad (2)$$

The $x^i[t+1]$ and $v^i[t+1]$ are the position and velocity of the particle “i” in the new iteration. The $x^{i,pbest}[t]$ shows the foremost position of particle” i”, and $x^{gbest}[t]$ represents the foremost position among the whole available particles. $r_1$ and $r_2$ are the random numbers between zero and one. $c_1$ and $c_2$ are positive constant parameters entitled acceleration coefficients. w is the inertia weight that is used to ensure convergence.

Figure 1 shows the flowchart algorithm for PSO [50].

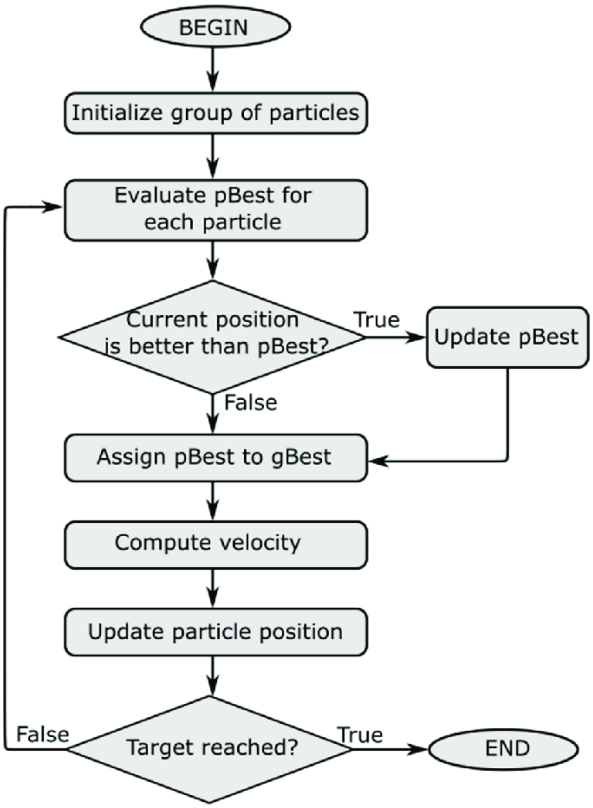


**Figure1. Flowchart algorithm for PSO**

The optimal amounts of the parameters w, $c_1$ and $c_2$ are obtained from the following relations. Table 2 specifies the implementation parameters of the PSO algorithm.

$$\chi = \frac{2\psi}{\emptyset - 2 + \sqrt{\emptyset^2 - 4\emptyset}} \quad (3)$$

$$\emptyset = \emptyset_1 + \emptyset_2 \quad (4)$$

$$w = \chi \quad (5)$$

$$c_1 = \chi\, \emptyset_1 \quad (6)$$

$$c_2 = \chi\, \emptyset_2 \quad (7)$$

In the above equations, $\emptyset_1$ and $\emptyset_2$ are constant values greater than zero, respectively, which must be adjusted to achieve the optimal value of the parameters of the PSO algorithm, including inertia weight (w), and learning coefficients ($c_1$ and $c_2$). Clerk suggested that if the values $\emptyset_1$ and $\emptyset_2$ were equal to 2.05 and the value of $\psi$ was considered equal to one, the optimal value of 0.73 for the inertia weight would be obtained [51]. The PSO is employed for data fitting issues, at which the variables are the required coefficients of the regression model for data fitting. In the case of a randomly initialized solution at the first iteration, the minimized error between the actual output value and predicted value can be calculated from the initialized solution to compute the fitting function. $a_0^{i.k}$, $a_1^{i.k}$, …., $a_n^{i.k}$ can be considered as the results of the PSO for i iteration and k population. The predicted output value related to $a_0^{i.k}$, $a_1^{i.k}$, …., $a_n^{i.k}$ for both the linear and non-linear regression models can be obtained using the following equations [52]:

$$y_{Predicted} = a_1^{i.k}x_1 + a_2^{i.k}x_2 + \cdots + a_n^{i.k}x_n + a_0^{i.k} \quad (8)$$

$$y_{Predicted} = a_n^{i.k}x_n + a_{n-1}^{i.k}x_{n-1} + \cdots + a_1^{i.k}x_1 + a_0^{i.k} \quad (9)$$

To generate the fitting function, one can use the minimizing of the equation 10 (cost function) by the PSO algorithm [53]:

$$E = \min[\sum(y_{actual} - y_{Predicted})^2] \quad (10)$$

**Table 2. Parameters of the PSO algorithm**

| Parameter | Value |
|---|---|
| Number of Iterations | 6000 |
| Population size | 300 |
| Mutation | 0.04 |
| Inertia weight (w) | 0.7298 |
| Personal learning coefficient($c_1$) | 1.4962 |
| General learning coefficient($c_2$) | 1.4962 |

**2.2. Data acquisition and analysis**

61 experimental data for gases at a pressure of 1 bar were gathered for this investigation [54-61]. The physical

properties of pure gases including temperature, critical temperature, critical pressure, molecular weight, viscosity, and heat capacity at constant volume were obtained for pure components and used for prediction of the conductivity of these gases. The Aspen Hysys V.11 software database was used to calculate viscosity and heat capacity at constant volume. The data collection used to create the model includes a variety of hydrocarbon and non-hydrocarbon compounds, some of which are listed in Table 3.

**Table 3. A list of the compounds utilized in the model's development**

| No. | Component | T(K) | $T_c$(K) | $P_c$(bar) | Mw | $\mu \times 10^7$(N.S.m$^{-2}$) | $C_v$(J.mol$^{-1}$.K$^{-1}$) |
|---|---|---|---|---|---|---|---|
| 1 | Acetone | 400 | 508.2 | 47.01 | 58.079 | 88.13 | 83.63 |
| 2 | Acetylene | 293 | 308.3 | 61.38 | 26.037 | 97.07 | 36.8 |
| 3 | Acetylene | 400 | 308.3 | 61.38 | 26.037 | 135.7 | 41.73 |
| 4 | Ammonia | 353 | 405.65 | 112.8 | 17.031 | 100.4 | 28.78 |
| 5 | Ammonia | 400 | 405.65 | 112.8 | 17.031 | 115.4 | 30.09 |
| 6 | Argon | 273.2 | 150.86 | 48.98 | 39.948 | 215.6 | 12.47 |
| 7 | Argon | 491.2 | 150.86 | 48.98 | 39.948 | 334.8 | 12.47 |
| 8 | Benzene | 400 | 562.05 | 48.95 | 78.112 | 95.9 | 103.8 |
| 9 | Carbon dioxide | 400 | 304.21 | 73.83 | 44.01 | 203.1 | 33.06 |
| 10 | Carbon dioxide | 473 | 304.21 | 73.83 | 44.01 | 244.2 | 35.08 |
| 11 | Carbon dioxide | 600 | 304.21 | 73.83 | 44.01 | 313 | 38.22 |
| 12 | Carbon dioxide | 1100 | 304.21 | 73.83 | 44.01 | 487.2 | 46.87 |
| 13 | Carbon dioxide | 1500 | 304.21 | 73.83 | 44.01 | 619.8 | 50.57 |
| 14 | Carbon monoxide | 91.88 | 132.92 | 34.99 | 28.01 | 59.52 | 21.16 |
| 15 | Carbon monoxide | 273 | 132.92 | 34.99 | 28.01 | 170 | 20.74 |
| 16 | Carbon monoxide | 291 | 132.92 | 34.99 | 28.01 | 178.6 | 20.76 |
| 17 | Carbon tetrachloride | 456.88 | 556.35 | 45.6 | 153.823 | 150.2 | 87.2 |
| 18 | Chlorine | 300 | 417.15 | 77.1 | 70.906 | 137.8 | 25.76 |
| 19 | Ethane | 239.11 | 305.32 | 48.72 | 30.069 | 75.54 | 38.18 |
| 20 | Ethane | 300 | 305.32 | 48.72 | 30.069 | 94.65 | 44.75 |
| 21 | Ethane | 500 | 305.32 | 48.72 | 30.069 | 156.8 | 69.3 |
| 22 | Ethyl alcohol | 373 | 514 | 61.37 | 46.068 | 76.78 | 69.15 |
| 23 | Ethylene | 250 | 282.34 | 50.41 | 28.053 | 85.51 | 32.12 |
| 24 | Ethylene | 273 | 282.34 | 50.41 | 28.053 | 93.27 | 33.75 |
| 25 | Ethylene | 300 | 282.34 | 50.41 | 28.053 | 100.24 | 35.78 |
| 26 | Ethylene | 400 | 282.34 | 50.41 | 28.053 | 136 | 44.05 |
| 27 | Ethylene | 500 | 282.34 | 50.41 | 28.053 | 167.6 | 52.88 |
| 28 | Ethylene | 600 | 282.34 | 50.41 | 28.053 | 195.7 | 61.59 |
| 29 | Helium | 144 | 5.2 | 2.275 | 4.003 | 109.9 | 12.48 |
| 30 | Helium | 273.2 | 5.2 | 2.275 | 4.003 | 598 | 12.48 |
| 31 | Heptane | 500 | 540.2 | 27.4 | 100.202 | 95.25 | 242.5 |
| 32 | Hydrogen | 250 | 33.19 | 13.13 | 2.016 | 74.66 | 20.01 |
| 33 | Hydrogen | 373 | 33.19 | 13.13 | 2.016 | 105.8 | 20.29 |
| 34 | Hydrogen | 450 | 33.19 | 13.13 | 2.016 | 122 | 20.48 |
| 35 | Hydrogen | 600 | 33.19 | 13.13 | 2.016 | 146.2 | 20.9 |
| 36 | Hydrogen | 800 | 33.19 | 13.13 | 2.016 | 178.2 | 21.52 |
| 37 | iso-Butane | 273 | 407.8 | 36.4 | 58.122 | 67.92 | 82.2 |
| 38 | iso-Butane | 373 | 407.8 | 36.4 | 58.122 | 94.13 | 109.2 |
| 39 | iso-Pentane | 373 | 460.4 | 33.8 | 72.149 | 84.32 | 136.4 |
| 40 | Methane | 200 | 190.564 | 45.99 | 16.042 | 78.24 | 25.06 |
| 41 | Methane | 300 | 190.564 | 45.99 | 16.042 | 113.4 | 27.74 |
| 42 | Methane | 400 | 190.564 | 45.99 | 16.042 | 144 | 32.33 |
| 43 | n-Butane | 273 | 425.12 | 37.96 | 58.122 | 65.85 | 82.7 |
| 44 | n-Butane | 400 | 425.12 | 37.96 | 58.122 | 98.6 | 116.2 |
| 45 | Neon | 373.2 | 44.4 | 26.53 | 20.18 | 425.7 | 12.49 |
| 46 | Nitric oxide | 200 | 180.15 | 64.8 | 30.006 | 134.7 | 21.28 |
| 47 | Nitrogen | 273 | 126.2 | 34 | 28.013 | 171.4 | 20.7 |
| 48 | Nitrogen | 400 | 126.2 | 34 | 28.013 | 226.4 | 21.37 |
| 49 | Nitrogen | 900 | 126.2 | 34 | 28.013 | 430.3 | 23.83 |
| 50 | Nitrous oxide | 273 | 309.57 | 72.45 | 44.013 | 130.7 | 29.31 |
| 51 | Oxygen | 173 | 154.58 | 50.43 | 31.999 | 128.8 | 19.56 |
| 52 | Oxygen | 200 | 154.58 | 50.43 | 31.999 | 147.5 | 19.84 |
| 53 | Oxygen | 350 | 154.58 | 50.43 | 31.999 | 237.7 | 21.38 |
| 54 | Oxygen | 500 | 154.58 | 50.43 | 31.999 | 307.7 | 22.84 |
| 55 | Propane | 250 | 369.83 | 42.48 | 44.096 | 68.22 | 57.38 |
| 56 | Propane | 273 | 369.83 | 42.48 | 44.096 | 74.7 | 61.79 |
| 57 | Propane | 300 | 369.83 | 42.48 | 44.096 | 82.27 | 66.94 |
| 58 | Propane | 373 | 369.83 | 42.48 | 44.096 | 103 | 80.6 |
| 59 | Propane | 400 | 369.83 | 42.48 | 44.096 | 110.9 | 85.53 |
| 60 | Propane | 500 | 369.83 | 42.48 | 44.096 | 140 | 103.1 |
| 61 | Sulfur dioxide | 273 | 430.75 | 78.84 | 64.064 | 107.4 | 30.46 |

**2.3. Selection of optimal configuration**

Three crucial characteristics that affect how well the constructed model performs are defined in this section. Each input data's correlation coefficient serves as the parameter [62]:

$$R^2 = 1 - \frac{\sum_{i=1}^{n}(k_{exp} - k_m)^2}{\sum_{i=1}^{n}(k_{exp} - \bar{k}_{exp})^2} \quad (11)$$

The second is the mean square error (MSE) [63]:

$$MSE = \frac{1}{n}\sum_{i=1}^{n}(k_{exp} - k_m)^2 \quad (12)$$

The third parameter is the mean relative error (MRE) [64]:

$$MRE = \frac{1}{n}\sum_{i=1}^{n}\left|\frac{k_{exp} - k_m}{k_{exp}}\right| \quad (13)$$

n is the number of data points, $k_{exp}$ is the experimental conductive heat transfer coefficient, $\bar{k}_{exp}$ is the average value of the experimental values and $k_m$ is the conductive heat transfer coefficient obtained from the modeling.

**3. Results**

Equation 14 was proposed to calculate the thermal conductivity coefficient of pure gases by the PSO algorithm:

$$A_1 = a_1 T^{a_2} P_r^{a_3} T_c^{a_4} Mw^{a_5} \mu^{a_6} C_v^{a_7} \quad (14)$$

$$A_2 = a_8 T^{a_9} P_r^{a_{10}} T_c^{a_{11}} Mw^{a_{12}} \mu^{a_{13}} C_v^{a_{14}} \quad (15)$$

$$A_3 = a_{15} T^{a_{16}} P_r^{a_{17}} T_c^{a_{18}} Mw^{a_{19}} \mu^{a_{20}} C_v^{a_{21}} \quad (16)$$

$$P_r = \frac{P}{P_c} \quad (17)$$

$$k_m = \frac{A_1 + A_2}{A_3} \quad (18)$$

**Table 4. Values for Calculation of $k_m$**

| i | $a_i$ | i | $a_i$ | i | $a_i$ |
|---|---|---|---|---|---|
| 1 | -0.4470 | 8 | 0.3294 | 15 | -0.4465 |
| 2 | -0.1780 | 9 | 0.3504 | 16 | -0.8012 |
| 3 | 0.0559 | 10 | 0.7352 | 17 | 0.2474 |
| 4 | -0.1045 | 11 | 0.1625 | 18 | 0.4298 |
| 5 | -0.0451 | 12 | 0.0490 | 19 | 0.6130 |
| 6 | -0.1607 | 13 | 0.0675 | 20 | -0.6132 |
| 7 | 0.5836 | 14 | 0.2522 | 21 | -0.1012 |

The cost function (equation 10) can be changed with iteration for the best model, as shown in Figure 2. It is clear that the cost function is almost equal to zero, which should be minimized.

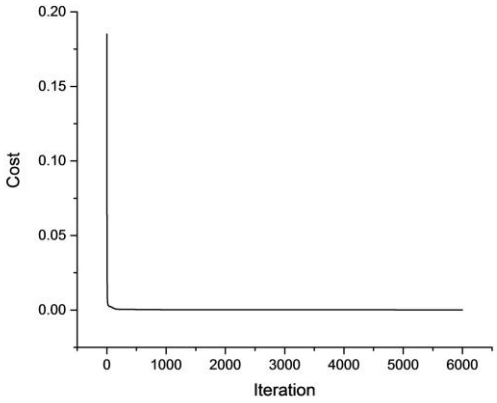


**Fig 2. A schematic of error variation during optimization**

The correlation between the simulation results and experimental data is illustrated in Figure 3.

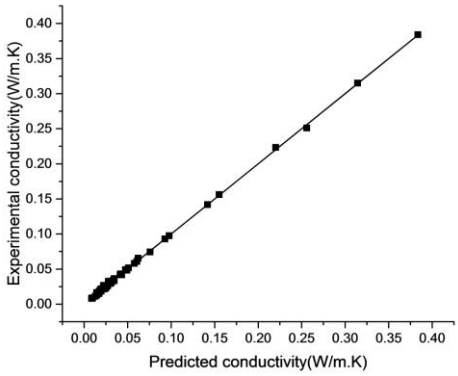


**Fig 3. Correlation of experimental data versus PSO predictions**

Table 5 shows the MRE, MSE and $R^2$ values calculated.

**Table 5. The MRE, MSE and $R^2$ values for the PSO configuration**

| MRE×100 | MSE×100 | $R^2$ |
|---|---|---|
| 4.67 | $2.4210 \times 10^{-4}$ | 0.9995 |

Table 6 shows the comparison of the proposed model with other correlations. The advantage of the proposed equation compared to other models is its simplicity.

**Table 6. Comparison of the proposed model with other correlations**

| No. | Component | T | Proposed Equation(RE× 100) | Other correlations(RE× 100) | Reference |
|---|---|---|---|---|---|
| 1 | Acetone | 400 | 3.23 | 6.96 | [65,66] |
| 2 | Acetylene | 293 | 6.44 | 2.29 | [65,66] |
| 3 | Acetylene | 400 | 4.28 | 0.00 | [65,66] |
| 4 | Ammonia | 353 | 2.33 | 17.94 | [68] |
| 5 | Ammonia | 400 | 5.08 | 16.48 | [68] |
| 6 | Argon | 273.2 | 10.50 | 1.84 | [67] |
| 7 | Argon | 491.2 | 16.44 | 0.74 | [67] |
| 8 | Benzene | 400 | 5.14 | 3.07 | [65,66] |
| 9 | Carbon dioxide | 400 | 4.60 | 0.81 | [67] |
| 10 | Carbon dioxide | 473 | 0.92 | 2.23 | [67] |
| 11 | Carbon dioxide | 600 | 2.93 | 6.77 | [67] |
| 12 | Carbon dioxide | 1100 | 1.90 | 12.23 | [67] |
| 13 | Carbon dioxide | 1500 | 0.49 | 0.61 | [22] |
| 14 | Carbon monoxide | 91.88 | 8.21 | 1.25 | [22] |
| 15 | Carbon monoxide | 273 | 8.04 | 7.23 | [67] |
| 16 | Carbon monoxide | 291 | 6.10 | 5.06 | [67] |
| 17 | Carbon tetrachloride | 456.88 | 14.62 | 1.40 | [68] |
| 18 | Chlorine | 300 | 7.56 | 5.61 | [67] |
| 19 | Ethane | 239.11 | 10.02 | 3.35 | [65,66] |
| 20 | Ethane | 300 | 5.06 | 1.83 | [65,66] |
| 21 | Ethane | 500 | 1.02 | 1.35 | [65,66] |
| 22 | Ethyl alcohol | 373 | 9.89 | 10.23 | [65,66] |
| 23 | Ethylene | 250 | 13.50 | 1.31 | [65,66] |
| 24 | Ethylene | 273 | 6.33 | 4.91 | [65,66] |
| 25 | Ethylene | 300 | 2.91 | 5.14 | [65,66] |
| 26 | Ethylene | 400 | 0.83 | 3.80 | [65,66] |
| 27 | Ethylene | 500 | 3.30 | 4.68 | [65,66] |
| 28 | Ethylene | 600 | 4.87 | 5.81 | [65,66] |
| 29 | Helium | 144 | 0.07 | 14.11 | [67] |
| 30 | Helium | 273.2 | 0.00 | 2.67 | [67] |
| 31 | Heptane | 500 | 14.13 | 0.61 | [65,66] |
| 32 | Hydrogen | 250 | 0.64 | 2.75 | [67] |
| 33 | Hydrogen | 373 | 1.38 | 3.44 | [67] |
| 34 | Hydrogen | 450 | 1.88 | 3.66 | [67] |
| 35 | Hydrogen | 600 | 0.22 | 5.77 | [67] |
| 36 | Hydrogen | 800 | 0.16 | 2.50 | [67] |
| 37 | iso-Butane | 273 | 7.06 | 5.79 | [65,66] |
| 38 | iso-Butane | 373 | 2.20 | 2.90 | [65,66] |
| 39 | iso-Pentane | 373 | 0.66 | 0.45 | [65,66] |
| 40 | Methane | 200 | 0.23 | 5.04 | [65,66] |
| 41 | Methane | 300 | 0.42 | 6.12 | [65,66] |
| 42 | Methane | 400 | 1.47 | 4.13 | [65,66] |
| 43 | n-Butane | 273 | 7.29 | 5.18 | [65,66] |
| 44 | n-Butane | 400 | 2.19 | 6.06 | [65,66] |
| 45 | Neon | 373.2 | 0.35 | 18.96 | [67] |
| 46 | Nitric oxide | 200 | 2.44 | 8.60 | [67] |
| 47 | Nitrogen | 273 | 6.18 | 5.21 | [67] |
| 48 | Nitrogen | 400 | 0.33 | 2.10 | [67] |
| 49 | Nitrogen | 900 | 0.11 | 7.24 | [67] |
| 50 | Nitrous oxide | 273 | 0.95 | 4.40 | [68] |
| 51 | Oxygen | 173 | 8.21 | 15.24 | [67] |
| 52 | Oxygen | 200 | 4.22 | 7.14 | [67] |
| 53 | Oxygen | 350 | 2.26 | 2.93 | [67] |
| 54 | Oxygen | 500 | 0.71 | 0.71 | [67] |
| 55 | Propane | 250 | 11.97 | 6.20 | [65,66] |
| 56 | Propane | 273 | 10.05 | 3.31 | [65,66] |
| 57 | Propane | 300 | 5.52 | 3.27 | [65,66] |
| 58 | Propane | 373 | 4.62 | 3.83 | [65,66] |
| 59 | Propane | 400 | 3.45 | 4.74 | [65,66] |
| 60 | Propane | 500 | 3.87 | 9.11 | [65,66] |
| 61 | Sulfur dioxide | 273 | 13.01 | 10.34 | [68] |
| 62 | Grand average | 91.88-1500 | 4.67 | 5.24 | - |

Table 7 shows the results of the equation test for several materials other than those listed in Table 3. The results of comparing the proposed equation with other equations show the high accuracy of the proposed equation for predicting the thermal conductivity coefficient for a wide range of materials.

**Table 7. Test of the proposed model**

| No. | Component | T | Proposed Equation(RE× 100) | Other correlations(RE× 100) | Reference |
|---|---|---|---|---|---|
| 1 | Acetonitrile | 353 | 18.62 | 22.00 | [55] |
| 2 | Acetonitrile | 393 | 14.29 | 19.00 | [55] |
| 3 | Cyclohexane | 353 | 2.75 | 4.20 | [55] |
| 4 | Cyclohexane | 433 | 6.40 | 9.00 | [55] |
| 5 | Ethyl ether | 273 | 6.32 | 3.10 | [55] |
| 6 | Ethyl ether | 373 | 6.43 | 11.00 | [55] |
| 7 | Ethyl ether | 486 | 12.62 | 13.00 | [55] |
| 8 | n-Hexane | 373 | 2.22 | 6.80 | [55] |
| 9 | n-Hexane | 433 | 8.38 | 9.40 | [55] |
| 10 | Grand average | 273-486 | 8.67 | 10.83 | - |

## 4. Conclusion

The thermal conductivity coefficient as one of the important parameters in the field of heat transfer from about 50 years ago up to now has been considered by scientists and researchers and has always tried to determine methods for measuring this parameter. In this work, 61 experimental data for pure gases at P=1 bar and variable temperature (91.88-1500 K) are collected. Then, using the PSO algorithm and MATLAB V2015 software, a simple equation for approximating the thermal conductivity is processed. During the validation phase, the suggested model attained the most accurate prediction with $R^2 = 0.9995$, MRE=4.67% and MSE=2.4210×$10^{-4}$%. The result of our study is advantageous for the simulation of different chemical processes based on gases through appropriate prediction of the thermal conductivity coefficient. It is important to mention that most of the previous models that were presented to determine the double thermal conductivity coefficient of gases have variables that require a lot of background knowledge and the number of their input variables is large, and they also have a lot of complexity to calculate. The advantage of the equation proposed in this research compared to other models is its simplicity.

## Notation

| | |
|---|---|
| $C_v$ | Heat capacity at constant volume $(J.mol^{-1}.K^{-1})$ |
| k | Conductive heat transfer coefficient $(W.m^{-1}.K^{-1})$ |
| Mw | Molecular Weight |
| P | Pressure (bar) |
| $P_c$ | Critical pressure (bar) |
| T | Temperature (K) |
| $T_c$ | Critical temperature (K) |
| μ | Viscosity (N.S.$m^{-2}$) |

## References


Ghassemi, M., Kamvar, M., & Steinberger-Wilckens, R. (2020). Fundamentals of heat and fluid flow in high temperature fuel cells. Academic Press.

Asadi, I., Shafigh, P., Hassan, Z. F. B. A., & Mahyuddin, N. B. (2018). Thermal conductivity of concrete–A review. Journal of Building Engineering, 20, 81-93.

Guildner, L. A. (1975). Thermal Conductivity of Gases. III. Some Values of the Thermal Conductivities of Argon, Helium, and Nitrogen from 0° C to 75° C at Pressures of 1× 105 to 2.5× 107 Pascals. Journal of research of the National Bureau of Standards. Section A, Physics and chemistry, 79(2), 407.

Ubbelohde, A. R. (1935). The thermal conductivity of polyatomic gases. The Journal of Chemical Physics, 3(4), 219-223.

Chapman, S., & Cowling, T. G. (1990). The mathematical theory of non-uniform gases: an account of the kinetic theory of viscosity, thermal conduction and diffusion in gases. Cambridge university press.

Hirsehfelder, J. O., Curtiss, C. F., & Bird, R. B. (1954). Molecular theory of gases and liquids. New York.

Longuet-Higgins, H. C., & Pople, J. A. (1956). Transport properties of a dense fluid of hard spheres. The Journal of Chemical Physics, 25(5), 884-889.

Longuet-Higgins, H. C., & Valleau, J. P. (1958). Transport coefficients of dense fluids of molecules interacting according to a square well potential. Molecular Physics, 1(3), 284-294.

Choh, S. T. (1958). The kinetic theory of phenomena in dense gases. University of Michigan.

Srivastava, B. N., & Barua, A. K. (1960). Thermal conductivity of binary mixtures of diatomic and monatomic gases. The Journal of Chemical Physics, 32(2), 427-435.

Davis, H. T., Rice, S. A., & Sengers, J. V. (1961). On the kinetic theory of dense fluids. IX. The fluid of rigid spheres with a square-well attraction. The Journal of Chemical Physics, 35(6), 2210-2233.

Bogoliubov, N. N., De Boer, J., & Uhlenbeck, G. E. (1962). Studies in statistical mechanics. Interscience, New York.

Horrocks, J. K., & McLaughlin, E. (1963). Non-steady-state measurements of the thermal conductivities of liquid polyphenyls. Proceedings of the Royal Society of London. Series A. Mathematical and Physical Sciences, 273(1353), 259-274.

Meixner, J. (1965). Statistical mechanics of equilibrium and non-equilibrium. Statistical Mechanics of Equilibrium and Non-equilibrium.

Sengers, J. V. (1966). Divergence in the Density Expansion of the Transport Coefficients of a Two-Dimensional Gas. The Physics of Fluids, 9(9), 1685-1696.

Mathur, S., Tondon, P. K., & Saxena, S. C. (1967). Thermal conductivity of binary, ternary and quaternary mixtures of rare gases. Molecular physics, 12(6), 569-579.

Tye, R. P., Hayden, R. W., & Spinney, S. C. (1977). Thermal conductivity of selected alloys at low temperatures. In Advances in Cryogenic Engineering (pp. 136-144). Springer, Boston, MA.

De Groot, J. J., Kestin, J., & Sookiazian, H. (1974). Instrument to measure the thermal conductivity of gases. Physica, 75(3), 454-482.

Healy, J. J., De Groot, J. J., & Kestin, J. (1976). The theory of the transient hot-wire method for measuring thermal conductivity. Physica B+ c, 82(2), 392-408.

Pliński, E. F., & Witkowski, J. S. (2001). Prediction of the thermal properties of CO2, CO, and Xe laser media. Optics & Laser Technology, 33(1), 61-66.

He, M. G., Liu, Z. G., & Yin, J. M. (2002). New equation of state for transport properties: calculation for the thermal conductivity and the viscosity of halogenated hydrocarbon refrigerants. Fluid Phase Equilibria, 201(2), 309-320.

Eslamloueyan, R., & Khademi, M. H. (2009). Estimation of thermal conductivity of pure gases by using artificial neural networks. International Journal of Thermal Sciences, 48(6), 1094-1101.

Gauthier, S., Giani, A., & Combette, P. (2013). Gas thermal conductivity measurement using the three-omega method. Sensors and Actuators A: Physical, 195, 50-55.

Ribeiro, V. G., Zabadal, J. G., Monticelli, C. O., & Borges, V. (2017). Estimating heat transfer coefficients for solid–gas interfaces using the Landau–Teller model. Applied Mathematics and Computation, 301, 135-139.

Lang, S., Pollak, S., & Frerich, S. (2019). Development of a method to measure the thermal conductivity of pressurised solutions containing dense gases using 11000 g/mol polydimethylsiloxane and carbon dioxide as example fluid. Fluid Phase Equilibria, 490, 92-100.

Cardona, L. F., & Valderrama, J. O. (2020). Physical and transport properties of ionic liquids using the geometric similitude concept and a cubic equation of state. Part 1: Thermal conductivity and speed of sound of pure substances. Journal of Molecular Liquids, 315, 113681.

Li, F., Shang, F., Cheng, S., Ma, W., Jin, H., Zhang, X., & Guo, L. (2020). Thermal conductivity measurements of the H2/CO2 mixture using the short-hot-wire method at 323.15–620.05 K and 2.14–9.37 MPa. International Journal of Hydrogen Energy, 45(55), 31213-31224.

Kim, D., Liu, H., Yang, X., Yang, F., Morfitt, J., Arami-Niya, A., ... & May, E. F. (2021). Thermal conductivity measurements and correlations of pure R1243zf and binary mixtures of R32+ R1243zf and R32+ R1234yf. International Journal of Refrigeration, 131, 990-999.

Liu, H., Yang, F., Yang, X., Yang, Z., & Duan, Y. (2021). Modeling the thermal conductivity of hydrofluorocarbons, hydrofluoroolefins and their binary mixtures using residual entropy scaling and cubic-plus-association equation of state. Journal of Molecular Liquids, 330, 115612.

Dehlouz, A., Jaubert, J. N., Galliero, G., Bonnissel, M., & Privat, R. (2022). Combining the entropy-scaling concept and cubic-or SAFT equations of state for modelling thermal conductivities of pure fluids. International Journal of Heat and Mass Transfer, 196, 123286.

Liu, Y., Wu, C., Zheng, X., & Li, Q. (2022). Modeling thermal conductivity of liquid hydrofluorocarbon, hydrofluoroolefin and hydrochlorofluoroolefin refrigerants. International Journal of Refrigeration.

Niksirat, M., Aeenjan, F., & Khosharay, S. (2022). Introducing hydrogen bonding contribution to the Patel-Teja thermal conductivity equation of state for hydrochlorofluorocarbons, hydrofluorocarbons and hydrofluoroolefins. Journal of Molecular Liquids, 351, 118631.

Rottmann, M., & Beikircher, T. (2022). Pressure dependent effective thermal conductivity of pure and SiC-opacified expanded perlite between 293 K and 1073 K. International Journal of Thermal Sciences, 179, 107652.

Yu, K., Wang, X., & Wang, Z. (2016). Multiple learning particle swarm optimization with space transformation perturbation and its application in ethylene cracking furnace optimization. Knowledge-Based Systems, 96, 156-170.

Cai, P., Nie, W., Chen, D., Yang, S., & Liu, Z. (2019). Effect of air flowrate on pollutant dispersion pattern of coal dust particles at fully mechanized mining face based on numerical simulation. Fuel, 239, 623-635.

Liu, Q., Nie, W., Hua, Y., Peng, H., Liu, C., & Wei, C. (2019). Research on tunnel ventilation systems: dust diffusion and pollution behaviour by air curtains based on CFD technology and field measurement. Building and Environment, 147, 444-460.

Vyazovkin, S., Burnham, A. K., Criado, J. M., Pérez-Maqueda, L. A., Popescu, C., & Sbirrazzuoli, N. (2011). ICTAC Kinetics Committee recommendations for performing kinetic computations on thermal analysis data. Thermochimica acta, 520(1-2), 1-19.

Parwekar, P., Rodda, S., & Vani Mounika, S. (2018). Comparison between genetic algorithm and PSO for wireless sensor networks. In Smart Computing and Informatics (pp. 403-411). Springer, Singapore.

Kennedy, J., & Eberhart, R. (1995, November). Particle swarm optimization. In Proceedings of ICNN'95-international conference on neural networks (Vol. 4, pp. 1942-1948). IEEE.

Buyukada, M. (2016). Co-combustion of peanut hull and coal blends: Artificial neural networks modeling, particle swarm optimization and Monte Carlo simulation. Bioresource Technology, 216, 280-286.

Song, C. (2011, July). Parameter estimation of the pyrolysis model for fir based on particle swarm algorithm. In 2011 Second International Conference on Mechanic Automation and Control Engineering (pp. 2354-2357). IEEE.

Safari, H., & Jamialahmadi, M. (2014). Thermodynamics, kinetics, and hydrodynamics of mixed salt precipitation in porous media: Model development and parameter estimation. Transport in porous media, 101(3), 477-505.

Farajnezhad, A., Afshar, O. A., Khansary, M. A., Shirazian, S., & Ghadiri, M. (2016). Correlation of interaction parameters in Wilson, NRTL and UNIQUAC models using theoretical methods. Fluid Phase Equilibria, 417, 181-186.

Moeini, P., & Bagheri, A. (2020). Adsorption kinetic modeling of toxic vapors on activated carbon in the batch reactor. Research on Chemical Intermediates, 46(12), 5547-5566.

de Paulo, E. H., Folli, G. S., Nascimento, M. H., Moro, M. K., da Cunha, P. H., Castro, E. V., ... & Filgueiras, P. R. (2020). Particle swarm optimization and ordered predictors selection applied in NMR to predict crude oil properties. Fuel, 279, 118462.

Troudi, H., Ghiss, M., Ben Guedria, N., Ellejmi, M., & Tourki, Z. (2022). A new Sauter mean diameter correlation suited for the gas cross flow in packed bed reactors based on PSO optimization algorithm. Separation Science and Technology, 1-24.

Farajpour, E., Behbahani, T. J., & Ghotbi, C. (2022). A new experimental and theoretical approach for viscosity Iranian heavy crude oils based on tuning friction theory and friction volume theory parameters. Inorganic Chemistry Communications, 139, 109319.

Eberhart, R., & Kennedy, J. (1995, October). A new optimizer using particle swarm theory. In MHS'95. Proceedings of the sixth international symposium on micro machine and human science (pp. 39-43). Ieee.

Zhang, Y., & Wu, L. (2011). A hybrid TS-PSO optimization algorithm. Journal of Convergence Information Technology, 6(5), 169-174.

Darvishi, R., Esfahany, M. N., & Bagheri, R. (2016). Numerical study on increasing PVC suspension polymerization productivity by using PSO optimization algorithm. International Journal of Plastics Technology, 20(2), 219-230.

Pranava, G., & Prasad, P. V. (2013, February). Constriction coefficient particle swarm optimization for economic load dispatch with valve point loading effects. In 2013 international conference on power, energy and control (ICPEC) (pp. 350-354). IEEE.

Rao, P. S., Varma, G. P., & Prasad, C. D. (2020, October). Identification of linear and non linear curve fitting models using particle swarm optimization algorithm. In AIP Conference Proceedings (Vol. 2269, No. 1, p. 030040). AIP Publishing LLC.

Rajpoot, V., Srivastava, D. K., & Saurabh, A. K. (2014). Optimization of I-shape microstrip patch antenna using PSO and curve fitting. Journal of Computational Electronics, 13(4), 1010-1013.

Green, D. W., & Southard, M. Z. (2019). Perry's chemical engineers' handbook. McGraw-Hill Education.

Reid, R. C., Prausnitz, J. M., & Poling, B. E. (1987). The properties of gases and liquids.

Robert, D. (1965). Thermal Conductivity of Gases and Liquids.

Eucken, A. (1911). On the temperature dependence of the thermal conductivity of several gases. Phys. Z, 12(1101-1107), 17.

Gregory, H. (1928). The thermal conductivities of oxygen and nitrogen. Proceedings of the Royal Society of London. Series A, Containing Papers of a Mathematical and Physical Character, 118(780), 594-607.

Mann, W. B., & Dickins, B. G. (1931). The thermal conductivities of the saturated hydrocarbons in the gaseous state. Proceedings of the Royal Society of London. Series A, Containing Papers of a Mathematical and Physical Character, 134(823), 77-96.

Gratch, S. (1950). Discussion:"New Measurements of the Heat Conductivity of Steam and Nitrogen"(Keyes, FG, and Sandell, Jr., DJ, 1950, Trans. ASME, 72, pp. 767–775). Transactions of the American Society of Mechanical Engineers, 72(6), 776-776.

Sherratt, G. G., & Griffiths, E. (1939). VI. A hot wire method for the thermal conductivities of gases. The London, Edinburgh, and Dublin Philosophical Magazine and Journal of Science, 27(180), 68-75.

Zhao, Z., Wang, J., Sun, B., Arowo, M., & Shao, L. (2018). Mass transfer study of water deoxygenation in a rotor–stator reactor based on principal component regression method. Chemical Engineering Research and Design, 132, 677-685.

Liu, Y., Hong, W., & Cao, B. (2019). Machine learning for predicting thermodynamic properties of pure fluids and their mixtures. Energy, 188, 116091.

Farzaneh-Gord, M., Rahbari, H. R., Mohseni-Gharesafa, B., Toikka, A., & Zvereva, I. (2021). Accurate determination of natural gas compressibility factor by measuring temperature, pressure and Joule-Thomson coefficient: Artificial neural network approach. Journal of Petroleum Science and Engineering, 202, 108427.

Misic, D., & Thodos, G. (1961). The thermal conductivity of hydrocarbon gases at normal pressures. AIChE Journal, 7(2), 264-267.

Misic, D., & Thodos, G. (1963). Atmospheric Thermal Conductivities of Gases of Simple Molecular Structure. Journal of Chemical and Engineering Data, 8(4), 540-544.

Bromley, L. A. (1952). Thermal conductivity of gases at moderate pressures. United States Atomic Energy Commission, Technical Information Service.

Stiel, L. I., & Thodos, G. (1964). The thermal conductivity of nonpolar substances in the dense gaseous and liquid regions. AIChE Journal, 10(1), 26-30.